Circular Dichroism in Multiphoton Ionization of Resonantly Excited He^{+} Ions

M. Ilchen, N. Douguet, T. Mazza, A. J. Rafipoor, C. Callegari, P. Finetti, O. Plekan, K. C. Prince, A. Demidovich, C. Grazioli, L. Avaldi, P. Bolognesi, M. Coreno, M. Di Fraia, M. Devetta, Y. Ovcharenko, S. Düsterer, K. Ueda, K. Bartschat, A. N. Grum-Grzhimailo, A. V. Bozhevolnov, A. K. Kazansky, N. M. Kabachnik, and M. Meyer

Phys. Rev. Lett. **118**, 013002 — Published 5 January 2017

DOI: 10.1103/PhysRevLett.118.013002

Circular Dichroism in Multiphoton Ionization of Resonantly Excited He^+ Ions

M. Ilchen[1,2], N. Douguet[3], T. Mazza[1], A. J. Rafipoor[1], C. Callegari[4], P. Finetti[4], O. Plekan[4], K. C. Prince[4,5,6], A. Demidovich[4], C. Grazioli[4], L. Avaldi[7], P. Bolognesi[7], M. Coreno[7], M. Di Fraia[8], M. Devetta[9], Y. Ovcharenko[1], S. Düsterer[10], K. Ueda[11], K. Bartschat[3], A. N. Grum-Grzhimailo[1,12], A. V. Bozhevolnov[13], A. K. Kazansky[14,15,16], N. M. Kabachnik[1,12,16], and M. Meyer[1]

[1] *European XFEL GmbH, Holzkoppel 4, 22869 Schenefeld Hamburg, Germany*
[2] *PULSE at Stanford, 2575 Sand Hill Road, Menlo Park, 94025 California, USA*
[3] *Department of Physics and Astronomy, Drake University, Des Moines, Iowa 50311, USA*
[4] *Elettra-Sincrotrone Trieste, I-34149 Basovizza, Italy*
[5] *Istituto Officina dei Materiali, Consiglio Nazionale delle Ricerche, Area Science Park, I-34149 Trieste, Italy*
[6] *Molecular Model Discovery Laboratory, Department of Chemistry and Biotechnology, Swinburne University of Technology, Melbourne, Victoria 3122, Australia*
[7] *CNR Istituto Struttura della Materia, Via del Fosso del Cavaliere, 100-00133 Roma, Italy*
[8] *Department of Physics, University of Trieste, I-34128 Trieste, Italy*
[9] *Istituto di fotonica e nanotecnologie CNR-IFN, Milano, Italy*
[10] *Deutsches Elektronen-Synchrotron (DESY), Notkestrasse 85, D-22603 Hamburg, Germany*
[11] *Institute of Multidisciplinary Research for Advanced Materials, Tohoku University, Sendai 980-8577, Japan*
[12] *Skobeltsyn Institute of Nuclear Physics, Lomonosov Moscow State University, Moscow 119991, Russia*
[13] *Sankt Petersburg State University, Universitetskaya nab. 7/9, Sankt Petersburg 199164, Russia*
[14] *Departamento de Fisica de Materiales, UPV/EHU, E-20018 San Sebastian/Donostia, Spain*
[15] *IKERBASQUE, Basque Foundation for Science, E-48011 Bilbao, Spain and*
[16] *Donostia International Physics Center (DIPC), E-20018 San Sebastian/Donostia, Spain*

(Dated: October 26, 2016)

Intense, circularly polarized extreme-ultraviolet (XUV) and near-infrared (NIR) laser pulses are combined to double-ionize atomic helium via the oriented intermediate $He^+(3p)$ resonance state. Applying angle-resolved electron spectroscopy, we find a large photon helicity dependence of the spectrum and the angular distribution of the electrons ejected from the resonance by NIR multiphoton absorption. The measured circular dichroism is unexpectedly found to vary strongly as a function of the NIR intensity. The experimental data are well described by theoretical modeling and possible mechanisms are discussed.

PACS numbers: 32.80.Fb, 32.80.Rm, 32.10.Dk

Dichroic phenomena in photoionization, i.e., the different response of a system to changes of the polarization state of the incoming light, have shown a high sensitivity to the dynamics of the underlying processes. Especially studies of the circular dichroism (CD), the different response to right- and left- circularly polarized light, have attracted much attention due to the possibility to investigate, for example, dichroic properties of electronic systems and chiral matter in general (e.g., [1, 2]). The interest ranges from fundamental spin control [3] to (bio-)chemistry [4] and material science such as magnetization studies [5]. The experimental work is often related to measurements using circularly polarized optical lasers or synchrotron radiation sources in combination with high-resolution angle-resolved electron spectroscopy. In earlier works (e.g., refs. [6–14] and references therein), the study of CD in photoelectron angular distributions revealed detailed information on atomic and molecular ionization, including the realization of a complete experiment, i.e., the determination of the photoionization amplitudes and their phases.

Dichroism in the strong field and multiphoton regime has been mainly investigated in the optical wavelength range. The extension of such studies to shorter wavelengths has become possible with the advent of Free-Electron Lasers (FELs) and their unprecedented intensity over a large photon energy range from soft to hard X-rays [15–17]. In particular, experimental investigations of the CD in two-color near-infrared (NIR) – extreme-ultraviolet (XUV) multiphoton ionization, which was predicted theoretically [18–20], only started recently [21, 22] with the operation of the seeded FEL FERMI [23], and even more recently with the installation of the Delta undulator at LCLS [24]. These FELs are capable of providing circularly polarized, ultra-intense XUV and X-ray pulses, respectively. In initial studies [21], the CD was found to be sensitive to details of the photoionization mechanism and the description of the continuum-continuum transitions involved. It is particularly informative to obtain the photoelectron angular distribution (PAD) [25–27] in order to determine the amplitudes of the photo-processes and their relative phases. The aim of this work is to develop a powerful and sensitive approach to study and control ionic resonances and their dichroic interaction with strong chiral fields.

In this Letter, we present a study where sequential double ionization and resonant two-color multiphoton ionization with circularly polarized pulses are applied together to the same system. The photoelectron spectra and the corresponding angular distributions arising from four-photon ionization of the XUV excited $He^+(3p)$ state by intense NIR pulses were investigated experimentally and theoretically for different relative helicities of the XUV and NIR radiation. The observed differences are attributed to the different angular momenta involved

in the two-color multiphoton process. The most unexpected observation is related to the strong NIR intensity dependence of the CD, which is mainly caused by a helicity dependent AC Stark shift for the magnetic sublevel of the $He^+(3p)$ resonance.

Our study is also related to the intriguing question whether the ionization probability of an electronic state with an electron (classically) co-rotating with the field is larger than in the counter-rotating case, and how the answer might depend on the laser parameters. For the non-adiabatic tunneling regime of strong-field ionization, it was predicted [28], on the basis of the semiclassical trajectory analysis of tunneling, and later confirmed experimentally [29] that the counter-rotating case is favored. In contrast, the co-rotating case dominates weak-field one-photon direct ionization [30, 31]. For multiphoton ionization of the $(n = 2)$ excited hydrogen atoms, it was predicted [32] that the co-rotating case is favored at small laser intensity, but at intensities higher than 10^{13} W/cm^2 the counter-rotating case starts to increasingly dominate. In all these cases only non-resonant multiphoton transitions were considered.

For the present study, we chose He atoms as target, in order to permit using a well-established computational approach. The scheme of our experiment is depicted in Fig. 1. A circularly polarized XUV pulse first ionizes the atom and produces a $He^+(1s)$ ion. The latter is then further excited by a second XUV photon to produce an oriented $He^+(3p, m = +1)$ intermediate state. Using a spatially overlapped and temporally synchronized pulse of circularly polarized NIR radiation, the $He^+(3p)$ state is finally ionized by four-photon absorption. The helicity of both pulses can be controlled. For fixed helicity of the XUV pulses, we investigated the CD by comparing results for opposite helicities of the NIR pulses.

In our case, the ionization proceeds in the multiphoton regime and hence the nomenclature of perturbation theory is appropriate. Already in lowest (non-vanishing) order perturbation theory (LOPT), there are many paths available to reach the continuum in the counter-rotating case, due to the different orbital angular momenta of the excited electron (see Fig. 1). Choosing the z-axis along the incident direction of the collinear XUV and IR pulses, the absorption (stimulated emission) of a photon with helicity $\mathcal{H} = +1$ increases (decreases) the magnetic quantum number m of the atom by one unit. A photon with helicity $\mathcal{H} = -1$ changes m in the opposite direction. Higher-order processes are also possible, with just a few indicated in the right part of Fig. 1. Further complications may occur by the third NIR photon coupling to high-lying Rydberg states of He^+ (not shown for clarity), although in the present setup the combined energy of three NIR photons would bring the unperturbed system just in between the $n = 6$ and $n = 7$ states, with a separation of 0.2 eV from each of these states, i.e., larger than the experimental energy uncertainty.

The experiments were performed at the Low Density Matter endstation (LDM) using the FEL-1 branch of the seeded free-electron laser FERMI [33]. The circularly polarized pulses of the FEL had a photon energy of 48.37 eV (25.63 nm), corresponding to the 10$^{\text{th}}$ harmonic of the FERMI seed laser. The bandwidth was determined to be $\approx$ 100 meV, which is sufficiently narrow to populate efficiently the $He^+(3p)$ state. The pulse duration (FWHM of the intensity) was 100 fs $\pm$ 20 fs, and an average pulse energy of 47 μJ $\pm$ 6 μJ was achieved at 10 Hz repetition rate of FERMI. The degree of circular polarization at LDM was $95\% \pm 5\%$, as determined earlier [21]. With a spot size of $50\,\mu$m $\pm$ $10\,\mu$m (FWHM) and 60% total transmission of the beamline, the He atoms were irradiated with a peak intensity of $\approx 1.0 \times 10^{13}$ W/cm^2 by the FEL. The central photon energy of the NIR laser was 1.58 eV (784 nm) with a bandwidth of $\approx$ 26 meV (13 nm) and a degree of polarization $> 99\%$. The pulse duration was $\approx$ 175 fs, and the average pulse energy was 604 μJ $\pm$ 1.5 μJ. With a spot size of $\approx$ 180 μm, the effective irradiation of the interaction region from this laser was $\approx 1.4 \times 10^{12}$ W/cm^2 for an optimized spatial overlap. The gaseous helium was injected into the center of a Velocity Map Imaging (VMI) electron spectrometer [33] where the FEL and NIR lasers were spatially and temporally overlapped. The energy resolution of the VMI was determined to be better than 100 meV from threshold to 4 eV, whereas the absolute kinetic energy accuracy was calibrated to be better than 200 meV. The electron emission patterns were reconstructed via Abel transformation [34].

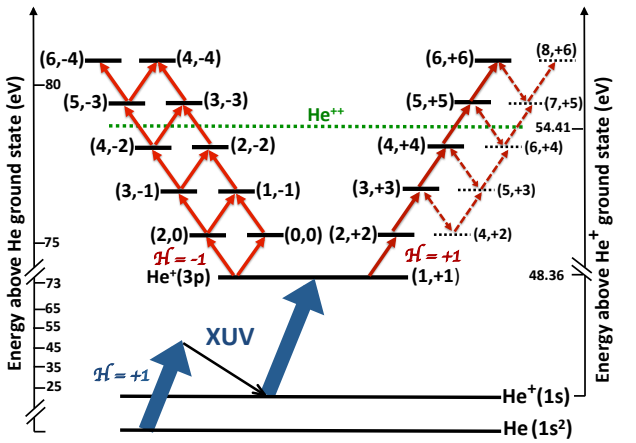

FIG. 1: (Color online) Scheme for sequential ionization of the neutral helium target. After the first FEL photon ($h\nu = 48.37$ eV) creates $He^+(1s)$, the sequential absorption of a second FEL photon produces the oriented $He^+(3p, m = +1)$ state. From here, the energy needed for ionization is provided by an NIR laser with a photon energy of 1.58 eV ($\lambda = 784$ nm) and changing helicities. The right branch corresponds to the co-rotating XUV and NIR fields, the left branch to the counter-rotating case. The solid lines associated with the optical laser indicate the possible pathways in LOPT. An illustration of higher-order processes is shown as dashed lines on the right side. Only the latter can, in principle, provide more than one possible path for the co-rotating case that predominantly reaches the $(\ell, m) = (5, +5)$ continuum at the lowest (main) peak and the $(6, +6)$ continuum in the first ATI peak.

The theoretical description of the present experiment is based on the two-step model of He sequential double ion-

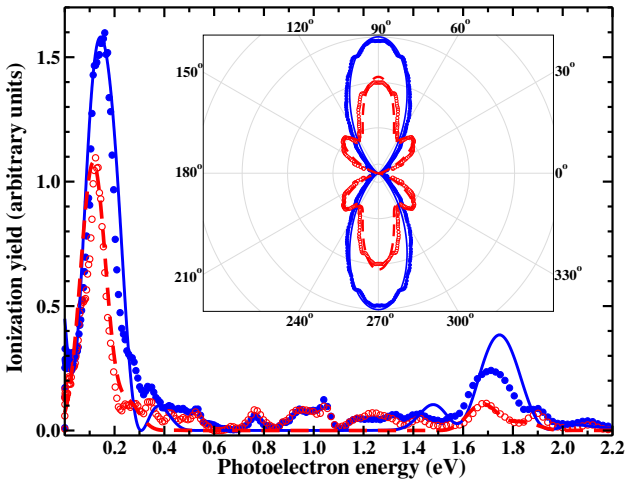

FIG. 2: (Color online) Experimental (symbols) and theoretical (lines) spectra of photoelectrons at an emission angle of $90° \pm 5°$ and angular distribution in the main photoelectron line (around 150 meV) for co-rotating (blue, solid circles and line) and counter-rotating (red, open circles and dashed line) circular polarizations in the lowest peak.

ization [35, 36], where the initial step of creating $He^+(1s)$ is decoupled from the subsequent excitation-ionization of the $He^+(3p)$ state. Then the non-relativistic time-dependent Schrödinger equation (TDSE) is solved numerically for the He^+ electron in the field of both the circularly polarized XUV and NIR pulses. For cross checking of the theoretical results we employed two independent computer codes to solve the TDSE [37, 38], which differ only in details. In the calculations, we assumed Gaussian pulses of about 22 fs in duration mainly due to limitations in computing power. The validity of comparing these results to the longer pulses of the experiment is given by the accurate match of both the spectrum and the angular distribution. Furthermore, a cross check of different pulse durations within the computing resources revealed no relevant differences to the results. The XUV and NIR pulses started at the same time, and the peak intensities were set to 1.0×10^{13} W/cm^2 for the XUV pulse and 1.4×10^{12} W/cm^2 for the NIR pulse, respectively.

The photoelectron spectra at the emission angles of $90° \pm 5°$ for the two cases of co-rotating and counter-rotating NIR and XUV circularly polarized pulses are displayed in Fig. 2. The prominent maximum at the photoelectron kinetic energy of ≈ 150 meV corresponds to four-NIR-photon ionization of the $He^+(3p)$ state, which was initially excited by the XUV pulse. Most importantly, the principal maxima for equal and opposite helicities exhibit a very strong difference ($\approx 40\%$) in their yields. A second clearly visible maximum at ≈ 1.75 eV is the ATI peak produced by the absorption of a fifth NIR photon.

The co-rotating and counter-rotating peaks reveal slightly different AC Stark shifts. This can be understood already within the LOPT. Indeed, the polarizability of the magnetic substate $(3p, m = +1)$ includes three terms: scalar, tensor, and axial [39]. While the AC Stark shift due to the first two is independent of the field helicity, the third term differs in sign for opposite helicities. This is supported by numerical calculations in second order perturbation theory [40].

In the inset of Fig. 2, the PADs are shown for the low-kinetic-energy peak for both relative helicities. Since the XUV and NIR beams are essentially collinear, the PADs are cylindrically symmetric with respect to the beam direction (z-axis). We present results in the plane containing this axis, which corresponds to $0°$ in the polar plot. The measured angular distributions are drastically different for the co-rotating and counter-rotating fields. In the former case, the PAD exhibits a simple shape, with just two lobes at $90°$ and $270°$, i.e., perpendicular to the beam direction. The distribution is more complex in the counter-rotating case, with four additional lobes at approximately $(2n-1) \times 45°$ for $n = 1, 2, 3, 4$.

The difference in the observed pattern can be qualitatively explained using the LOPT (see Fig. 1). For the co-rotating case, only the partial wave $l = 5$ with $m = +5$ contributes to the lowest peak, i.e., the PAD is predominantly determined by $|Y_{5,+5}(\theta, \phi)|^2 \sim \sin^{10}\theta$. For counter-rotating fields, on the other hand, at least two partial waves, $l = 5$ and $l = 3$ contribute, both with $m = -3$. The more complex PAD in this case is thus determined by the absolute square of a superposition of $Y_{5,-3}(\theta, \phi)$ and $Y_{3,-3}(\theta, \phi)$, which includes an interference term. For both cases, co-rotating and counter-rotating fields, the remaining channels contribute less than 0.1% to the main peak.

The CD is defined as $[P_+ - P_-]/[P_+ + P_-]$, where P_+ and P_- are the probabilities for ionization by circularly polarized pulses with the same $(+)$ or opposite $(-)$ helicity, respectively. The angle-integrated values of the CD at 1.4×10^{12} W/cm^2 are $0.169^{+0.06}_{-0.10}$ for the experiment and 0.244 for theory. In addition, we recorded angularly resolved electron emission data and derived the angle-integrated CD under reduced effective NIR intensity of 7.3×10^{11} W/cm^2 [21]. For this setting, the experimental integral CD value is $0.98^{+0.02}_{-0.11}$, while the TDSE calculations yield 0.95.

The dominating ionization by co-rotating fields at low intensities, leading to an exceptionally large positive CD, can again be qualitatively understood in terms of the LOPT. The right branch in Fig. 1 (co-rotating fields) to $(l = 5, m = +5)$ contains only a single path with four dipole transitions of the type $(l, m = l) \rightarrow (l+1, m = l+1)$, which are most favorable among the dipole transitions with increasing l. The left branch (counter-rotating fields) contains a path to $(l = 5, m = -3)$ with a probability (estimated from angular factors alone) $\frac{735}{16} \approx 50$ times smaller than the right branch. Excitation of $(l = 3, m = -3)$ is more complicated. This can be reached in LOPT by four interfering paths, involving different combinations of intermediate states with various l. Due to smaller angular factors and likely some destructive interference between the amplitudes of these paths, the ionization probability into $(l = 3, m = -3)$ is expected to be much smaller than for $(l = 5, m = +5)$. For the NIR intensity of 7.3×10^{11} W/cm^2 our qualitative conclusions are

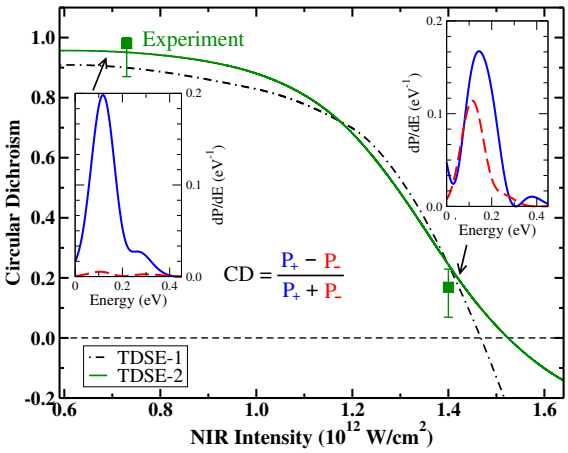

FIG. 3: (Color online) Circular dichroism in the peaks at 200 meV as function of the NIR peak intensity for an XUV peak intensity of 1.0×10^{13} W/cm^2. The two experimental points are compared with predictions from the TDSE calculations (TDSE-1 [37], TDSE-2 [38]). The insets show the low-energy spectra from the TDSE calculations for the two experimental cases.

supported by the TDSE calculations, resulting in the probabilities $P_{5,5} = 1.5{\cdot}10^{-2}$, $P_{5,-3} = 2.7{\cdot}10^{-4}$, $P_{3,-3} = 2.3{\cdot}10^{-4}$, with almost two orders of magnitude difference in the ionization probability for co- and counter-rotating fields.

Figure 3 shows the angle-integrated CD of the low-kinetic-energy peak as a function of the NIR intensity. With increasing NIR intensity, the CD decreases and is predicted to even change sign at $I_{\rm NIR} \gtrsim 1.5 \times 10^{12}$ W/cm^2, i.e., ionization by counter-rotating fields becomes more effective.

The question, therefore, arises how such a relatively small change of the NIR intensity, well in the multiphoton regime, can possibly cause such a large change in the measured CD. In this regard, Fig. 4 shows the population of the $\mathrm{He}^+(1s)$ and $\mathrm{He}^+(3p, m = +1)$ states at the end of the laser pulses. The population of the $3p$ state is very high for low NIR intensities, for both the co-rotating and the counter-rotating cases. This simply confirms the desired, very high likelihood for the second XUV photon to excite the He^+ ion. Since the co-rotating case is favored due to angular-momentum factors and pretty much protected from destructive interference, the $(3p, m = +1)$ state is much more efficiently ionized in this case than in the counter-rotating case. Hence, the measured CD is close to unity at the relatively low NIR peak intensity of $0.6{\times}10^{12}$ W/cm^2, even though there are already about 25% fewer $\mathrm{He}^+(3p, m = +1)$ ions available for ionization than for the counter-rotating case.

When the NIR intensity is increased, however, it causes the $(3p, m = +1)$ state to shift slightly for the co-rotating cases, as seen by the change in energy of the peak in the inserts of Fig. 3. This small shift is nevertheless sufficient to significantly reduce (by almost an order of magnitude) the $\mathrm{He}^+(3p, m = +1)$ population that is available for subsequent four-photon NIR ionization. The vast majority of atoms stay in the ground state $\mathrm{He}^+(1s)$. In contrast, the $\mathrm{He}^+(3p, m = +1)$ population is hardly affected in the counter-rotating scenario. Consequently, the less-favored path rapidly picks up in importance, thereby reducing the measured CD substantially.

While we cannot rule out other mechanisms that might contribute to this apparently complex situation, the above scenario seems valid. It is also supported by the fact that the ionization probability for the co-rotating case (the area under the curve) hardly increases when the NIR intensity is doubled (see inserts of Fig. 3). In the simplest scenario, one would have expected an increase by about a factor of $2^4 = 16$, but this expected increase is compensated for by the accompanying decrease in the available $\mathrm{He}^+(3p, m = +1)$ ions.

In conclusion, by applying a circularly polarized XUV pulse to the He^+ ground state, we deliberately excited the ion to the $m = +1$ magnetic sublevel of the $3p$ state. This excited and oriented state was then ionized by a co-rotating or counter-rotating NIR field. Employing a circularly polarized NIR laser and obtaining the corresponding circular dichroism of the ejected electron from the resonance provides a novel approach to determine electronic orientation in ionic resonances in general. Varying the NIR intensity, the resonant absorption probability can furthermore be controlled due to a dichroic AC Stark shift.

We revealed experimentally and supported by calculations that the measured circular dichroism depends to a surprisingly strong extent on the peak intensity of the NIR field for a fixed XUV pulse. At small NIR intensities, the CD is positive and close to unity. With increasing NIR intensity, the CD is calculated to become negative. The intensity dependence of CD predicted in previous studies [28, 32] is much smoother and the zero-crossing occurs at about one order of magnitude higher intensity than in the present case. In our case of multiphoton ionization via an intermediate resonant state, the reason is a different helicity-dependent shift of the $\mathrm{He}^+(3p, m = \pm 1)$ states due to the presence of the circularly polarized NIR field. Even though the dynamic AC Stark shift in the electron spectra is determined to be small, it appears to be sufficient to significantly affect the initial population of the excited He^+ ions that are available for subsequent ionization.

The technique discussed in this Letter is directly applicable to any FEL source with polarization control and to any

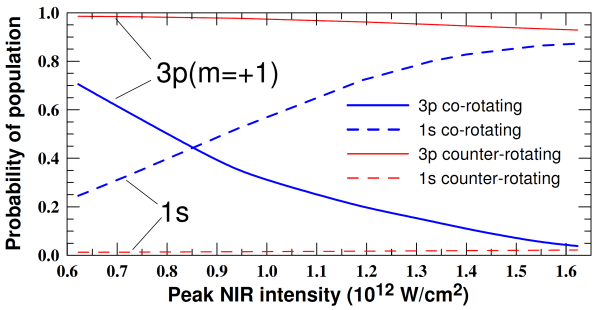

FIG. 4: (Color online) TDSE predictions for the populations of $\mathrm{He}^+(1s)$ and $\mathrm{He}^+(3p, m = +1)$ for the co- and counter-rotating cases at the end of the pulses as a function of the NIR peak intensity.

atomic, molecular, or solid-state target. Future projects on the dynamics of oriented states or structurally chiral targets and the manipulation of magnetization via pre-oriented spins of inner-shell electrons excited, for example, in conduction bands, are expected to greatly benefit from the new handle on circular dichroism control presented here.

The authors acknowledge the invaluable support of the technical and scientific staff of FERMI at Elettra-Sincrotrone Trieste. We also thank J. Viefhaus, DESY, for fruitful discussions. M.I. acknowledges funding from the Volkswagen Foundation, M.I. and A.J.R. received financial support from SFB 925 "Light induced dynamics and control of correlated quantum systems" at the University of Hamburg, T.M. and M.M. acknowledge financial support by Elettra within the CALIPSO Transnational Access Programme, and N.M.K. was supported by the European XFEL, DIPC, and the programme "Physics with Accelerators and Reactors in Western Europe" of the Russian Ministry of Education and Science. A.N.G. acknowledges support by the European XFEL. N.D. and K.B. acknowledge funding by the United States National Science Foundation under grant No. PHY-1403245 and the XSEDE supercomputer allocation No. PHY-090031 to access Stampede at the Texas Advanced Computing Center and SuperMIC at Louisiana State University.

[1] G. A. Garcia *et al.*, *Nat. Commun.* **4**, 2132 (2013).
[2] M. Pitzer, *et al.*, *Science* **341**, 1096 (2013).
[3] C. E. Graves *et al.*, *Nat. Mater.* **12**, 293 (2013).
[4] N. J. Greenfield, *Nat. Protoc.* **1**, 2876 (2007).
[5] C. von Korff Schmising, *et al.*, *Phys. Rev. Lett.* **112**, 217203 (2014).
[6] P. Lambropoulos, *Phys. Rev. Lett.* **28**, 585 (1972).
[7] R. L. Dubs, S. N. Dixit, and V. McKoy, *J. Chem. Phys.* **85**, 656 (1986).
[8] D. J. Leahy *et al.*, *J. Chem. Phys.* **97**, 4948 (1992).
[9] S. Cavalieri *et al.*, *Phys. Rev. A* **47**, 4219 (1993).
[10] C. S. Feigerle *et al.*, *Phys. Rev. A* **53**, 4183 (1996).
[11] G. Schönhense and J. Hormes, in *VUV and Soft X-ray Photoionization*, eds. U. Becker and D. A. Shirley (Plenum Press, New York, 1996).
[12] Z. M. Wang *et al.*, *Phys. Rev. Lett.* **84**, 3795 (2000).
[13] N. Böwering *et al.*, *Phys. Rev. Lett.* **86**, 1187 (2001).
[14] L. Nahon *et al.*, *Phys. Chem. Chem. Phys.* **18**, 12696 (2016).
[15] W. Ackermann *et al.*, *Nat. Photon.* **1**, 336 (2007).
[16] P. Emma *et al.*, *Nat. Photon.* **4**, 641 (2010).
[17] T. Ishikawa *et al.*, *Nat. Photon.* **6**, 540 (2012).
[18] N. L. Manakov, *et al.*, *J. Phys. B* **32**, 3747 (1999).
[19] R. Taieb, V. Veniard, A. Maquet, N. L. Manakov, S. I. Marmo, *Phys. Rev. A* **62**, 013402 (2000).
[20] A. K. Kazansky, A. V. Grigorieva, and N. M. Kabachnik, *Phys. Rev. Lett.* **107**, 253002 (2011).
[21] T. Mazza, *et al.*, *Nat. Commun.* **5**, 3648 (2014).
[22] G. Hartmann, *et al.*, *Rev. Scientific Instr.* **87**, 083113 (2016).
[23] E. Allaria, *et al.*, *Phys. Rev. X* **4**, 041040 (2014).
[24] A. A. Lutman, *et al.*, *Nat. Phot.* **10**, 1038 (2016).
[25] S. Mondal *et al.*, *J. Phys. B* **46**, 205601 (2013).
[26] L. H. Haber, B. Doughty, and S. R. Leone, *Phys. Rev. A* **79**, 031401 (2009).
[27] T. Mazza, *et al.*, *J. Mod. Opt.* **63**, 367 (2016).
[28] I. Barth and O. Smirnova, *Phys. Rev. A* **84**, 063415 (2011).
[29] T. Herath, L. Yan, S. K. Lee, and W. Li *Phys. Rev. Lett.* **109**, 043004 (2012).
[30] H. Bethe, *Intermediate Quantum Mechanics* (W. A. Benjamin Inc. New York, 1964).
[31] S. Askeland, S. A. Sorngard, I. Pilskog, R. Nepstad, and M. Forre *Phys. Rev. A* **84**, 033423 (2011).
[32] J. Bauer, *et al.*, *Phys. Rev. A* **90**, 063402 (2014).
[33] V. Lyamayev, *et al.*, *J. Phys. B* **46**, 164007 (2013).
[34] M. J. J. Vrakking, *Rev. Sci. Instrum.* **72**, 4084 (2001).
[35] S. Fritzsche, A. N. Grum-Grzhimailo, E. V. Gryzlova, and N. M. Kabachnik *J. Phys. B* **41**, 165601 (2008).
[36] A. N. Grum-Grzhimailo, E. V. Gryzlova, S. Fritzsche, and N. M. Kabachnik *J. Mod. Opt.* **63**, 334 (2016).
[37] A. K. Kazansky and N. M. Kabachnik *J. Phys. B* **40**, 2163 (2007).
[38] N. Douguet, A. N. Grum-Grzhimailo, E. V. Gryzlova, E. I. Staroselskaya, J. Venzke, K. Bartschat, *Phys. Rev. A* **93**, 033402 (2016).
[39] N. B. Delone and V. P. Krainov, *Multiphoton Processes in Atoms*, 2nd edn. (Springer, Heidelberg, 2000).
[40] M. Gajda, B. Piraux, K. Rzazewski *Phys. Rev. A* **50**, 2528 (1994).